Non-coherent Signal Detection and Bit Error Rate for an Ambient Backscatter Link under Fast Fading

J. Kartheek Devineni and Harpreet S. Dhillon

***Abstract*—Non-coherent detection is an important component of ambient backscatter communication due to the energy constrained nature of the backscatter devices. This paper provides the first comprehensive performance analysis of non-coherent detection under a fast-varying wireless channel for ambient backscatter communication. In particular, we evaluate the bit error rates (BERs) for two data encoding mechanisms under a new receiver architecture that is based on the direct averaging of the received signal samples. Our results concretely demonstrate the existence of BER floor for a single antenna receiver, which results in poor performance. We further show that a multi-antenna receiver can overcome this drawback by eliminating the interference created by the direct link from the ambient power source that considerably improves the BER of this receiver. This multi-antenna receiver exploits the fact that the time duration of the variation in angle of arrival (AoA) of the communication links in the fast-varying channel is much larger than the coherence period of the small-scale fading, allowing it to track the AoA of the direct link.**

***Index Terms*—Ambient backscatter, non-coherent detection, fast fading, multiple antennas, BER.**

I. Introduction

Ambient backscatter systems are playing an increasingly important role in the development of machine-to-machine (M2M) communications, an enabling technology of the Internet-of-Things (IoT) paradigm. As a consequence of the services rendered by these networks, many of these devices are required to be deployed in a variety of challenging and diverse conditions. For example, a large portion of them will be installed in high mobility vehicles for relaying traffic and other crucial information. Due to the large Doppler spread, the propagation channel could vary very quickly in these cases, thereby making the channel estimation and tracking procedures extremely challenging to implement. The fast-varying nature of the channel means that the transmission and detection schemes used in slow fading channels are unsuitable for these scenarios [1]. Interestingly, the current literature on ambient backscatter is devoid of studies focusing on fast fading channels. Therefore, in this paper, we address this limitation by exploring transmission and detection mechanisms under fast fading channels and mathematically characterizing their BER performance.

Prior Art: As noted above, the existing literature on ambient backscatter systems is limited to the slow fading channels [1]–[12]. The exact BER analysis of ambient backscatter systems along with a detailed overview of the backscatter concept is provided in [1]. Maximum-likelihood (ML) detection in an ambient backscatter setup was first investigated in [2]. The signal detection under non-coherent and semi-coherent setups is analyzed in [3]–[6]. The signal detection at a multi-antenna receiver is studied in [7] and the statistical-covariance based detection is explored in [8]. Apart from [1], the other works [1]–[8] are approximation based, using Gaussian distribution as the model for the conditional distributions of the average energy of the received signal. Ambient backscatter communication using orthogonal frequency division multiplexing (OFDM) is investigated in [9], [10]. On the same lines [11], [12] explored new coding schemes, such as Manchester coding, to improve detection. To the best of our knowledge, this is the first work that incorporates the fast fading channel into an ambient backscatter setup.

Setup and Contributions: Assuming fast fading, we study the non-coherent detection of ambient backscatter system for two different receivers; one with a single antenna and the other with multiple antennas. The number of antenna elements are assumed to be two for the second case. Two types of data encoding schemes are employed at the transmitter, of which, the first scheme $\mathcal{M}_1$ directly transmits the message bit using on-off keying (OOK) modulation, and the second scheme $\mathcal{M}_2$ transmits either codeword $[0\,1]$ or $[1\,0]$ (depending on the value of the message bit) using OOK modulation over two symbol durations. The encoding used in $\mathcal{M}_2$ is one of the standard schemes used for non-coherent detection in the literature [13]. Our main contributions in this paper are: 1) non-coherent detection of an ambient backscatter system, 2) detection architecture based on the average of received signal samples instead of the average received signal energy, and 3) improving BER of this receiver architecture for the two encoding schemes using multiple antennas in a fast fading channel. For a single antenna receiver, we demonstrate that the system reaches BER floor very quickly, which is mainly attributed to the interference created by the direct link from the ambient power source. Therefore, the purpose of using multiple antennas at the receiver in our work is to eliminate interference created by this direct link. The novelty of this approach lies in the ability of the multi-antenna receiver to take advantage of the fact that the variation in the AoA of the links is much slower than the temporal variation of the overall channel. The BER results demonstrate the substantial improvement in performance of the receiver when multiple antennas are used.

II. System Model

We consider a spatially correlated flat Rayleigh fading channel with coherence time of the same order as the symbol

J. K. Devineni and H. S. Dhillon are with Wireless@VT, Department of ECE, Virginia Tech, Blacksburg, VA (email: kartheekdj@vt.edu and hdhillon@vt.edu).
This work was supported by the US NSF under Grant CPS-1739642.

duration of data carried by the ambient radio frequency (RF) wave. The impulse response of this channel can be expressed as:

$$\vec{h}(t) = \underbrace{\sum_i c_i e^{j\phi_i - j2\pi c\tau_i/\lambda + j2\pi f_d \cos\psi_i t}\, \vec{a}(\theta_0)}_{h_0} \delta\left(t-\bar{\tau}\right), \quad (1)$$

where θ_0 is the AoA of the dominant non-line-of-sight (NLOS) path with i independent sub-paths, $\vec{a}(.)$ is the antenna array response vector at the receiver, c_i is the sub-path gain, ϕ_i is the phase of the sub-path which is taken to be uniformly distributed in $[0, 2\pi)$, τ_i is the time delay of the sub-path, f_d is the maximum Doppler spread, and ψ is the angle of departure (AoD) of the sub-path at the transmitter. The envelope of the resulting channel coefficient h_0 can be characterized as a Rayleigh distributed random variable (RV) by invoking the central limit theorem (CLT) for the independent sub-paths. Interested readers can refer to the expanded version [14] of this paper for an illustration of this channel model. This environment is close to many real-world scenarios, such as when a moving mobile user is used as a power source by a transmitter to communicate with a receiver which can be either a base station (BS) or another backscatter device. The variation of h_0 with time is dependent on the Doppler spread f_d and the angular spread ψ_i at the mobile user, which in this case are assumed to be high due to the speed of the user and the presence of local scatterers. On the other hand, $\vec{a}(.)$ is dependent on the AoA θ_0, the time-scale over which the vector evolves is several orders of magnitude larger compared to the coherence time of h_0, and hence can be tracked by the system. This means that while the channel coefficient at the receiver will be changing for each symbol of the ambient data, the angular variation corresponding to AoA of the received signal will not change at the same order and can be assumed to be constant over few symbol periods. In a multi-antenna receiver, this will be used to improve the BER performance of the system. More information on this channel model can be found in [15]–[17].

Remark 1. *Typically, the channel coefficients are correlated for a few consecutive symbol periods even at a large Doppler spread of the fading channel. However, for the ease of exposition, the channel coefficients are assumed to be independent over each symbol duration of the ambient RF data.*

Remark 2. *The assumption of spatially correlated channel at the receiver is typically valid for a BS located above the rooftops as the angular spread is small in these scenarios. We assume this to be valid for a backscatter device too by considering a single dominant NLOS path. Handling the case of multiple angular paths at the receiver is left as a future work.*

A. Signal Model

The ambient backscatter setup considered in this paper consists of three devices: ambient power source, backscatter transmitter (BTx), and receiver (Rx). For concreteness, the ambient power source in the work is assumed to be a single antenna transmitter. However, even if multiple antennas are used, for example to beamform the signal, it would only change the power gain at the receiver. The power gain is a function of the antenna array factor and the angular position of the backscatter Tx-Rx pair, where the gain increases and decreases if the pair is located inside and outside the angular zone of the intended receiver respectively. This would not directly affect our analysis since the power gain of the signal is a large-scale parameter which would be absorbed into the signal to noise ratio (SNR) of the ambient signal. At the receiver, the signal scattered from the backscatter device is given by [18]:

$$r = (A - \Gamma)\, s = As - \Gamma s, \quad (2)$$

where r is the signal at the receiver, s is the signal backcattered at the device, A is the load-independent complex coefficient of the device, and Γ is the reflection coefficient of backscatter node at the boundary of the antenna and the circuit. We assume that the transmitter uses a simple binary on-off modulation scheme to transmit the digital data, which is a common choice for backscatter systems. The binary OOK modulation scheme can be implemented by choosing two different values Γ_0 and Γ_1. It is possible to achieve the OOK modulation for antennas with $|A| \leq 1$ by designing the appropriate load impedance using only passive components such as resistors, capacitors, and inductors [19], [20].

We make the assumption that the rate of backscatter data is significantly lower than the rate of ambient RF data (reasonable for most IoT applications), which allows us to represent the backscatter data as a single variable b, for a window of N received signal samples. For a Rx with single antenna, the received signal is composed of two components, one directly received from the power source and the other reflected from the BTx. This can be mathematically represented as follows:

$$y(n) = \underbrace{h_r(n)x(n)}_{\text{radio signal}} + \underbrace{\alpha b\; h_b(n)\; h_t(n)x(n)}_{\text{backscatter signal}} + \underbrace{w(n)}_{\text{AWGN}}, \quad (3)$$

where $x(n)$ is the ambient radio signal in complex baseband form, $w(n)$ is the zero mean additive complex Gaussian noise with a variance of σ_n^2, $h_r(n), h_b(n)$ and $h_t(n)$ are zero mean complex Gaussian channel coefficients with a variance of σ_h^2, $b \in \{0, 1\}$ is the backscatter data and α is related to the parameter Γ_1 of the BTx node. This received signal can be easily modified for a dual-antenna Rx as follows:

$$\begin{aligned}\mathbf{y}(n) = \begin{bmatrix} y_0(n) \\ y_1(n) \end{bmatrix} &= h_r(n) \begin{bmatrix} 1 \\ e^{j\phi_1} \end{bmatrix} x(n) \\ &+ \alpha b\; h_b(n)h_t(n) \begin{bmatrix} 1 \\ e^{j\phi_2} \end{bmatrix} x(n) + \begin{bmatrix} w_0(n) \\ w_1(n) \end{bmatrix}, \end{aligned} \quad (4)$$

where $\phi_i \equiv \frac{2\pi}{\lambda} d \cos\theta_i$ is the phase offset between the two antenna elements which is dependent on AoA θ_i. Note that the AoA θ_2 of the backscatter link is independent from the AoA θ_1 of the direct link.

As is the case with many modulation schemes of interest, we assume that the energy of the ambient sequence $x(n)$ over N samples averages out to a constant which is given by

$$\bar{E} = \frac{1}{N} \sum_{n=1}^{N} |x(n)|^2. \quad (5)$$

Also, the ambient symbols $x(n)$ are assumed to be an independent and identically distributed (i.i.d.) sequence.

The receiver architecture used for detection in [1], and

other works focusing on slow fading channels, is based on the energy averaging of the received signal samples. The reason is that directly averaging the received signal to generate $Y = \frac{1}{N}\sum_{n=1}^{N} y(n)$ will result in exactly the same conditional distributions for Y under both of the hypotheses, due to which it is not possible to differentiate the constellation points of different bits. For the non-coherent detection in the paper, we employ this architecture to detect the backscatter data. We concretely demonstrate that the architecture by itself is inadequate for a single-antenna receiver by deriving BER for this non-coherent setup. We further show that this architecture can be used in conjunction with multiple antennas at the receiver and eliminate the strong interference generated by the direct link from the power source.

III. Signal Detection and Bit Error Rate

Before describing the detection with a multi-antenna receiver, we derive the conditional signal distributions and perform detection with a single-antenna receiver. This approach allows us to demonstrate the poor BER performance of a single-antenna receiver, which can be overcome by utilizing multiple antennas at the receiver for this particular fast fading channel.

A. Conditional Signal Distributions

For scheme $\mathcal{M}_1$, the null hypothesis $\mathcal{H}_0$ and the alternate hypothesis $\mathcal{H}_1$ correspond to the scenarios with backscatter data $b \equiv 0$ and $b \equiv 1$ (which also correspond to the transmitted message bit $m \equiv 0$ and $m \equiv 1$ in this case), respectively. As described earlier, the receiver architecture is based on the averaging of the received signal samples which is represented by the variable Y.

Lemma 1. *The probability density functions (PDFs) of Y conditioned on $\mathcal{H}_0$ and $\mathcal{H}_1$ for the scheme $\mathcal{M}_1$ are characterized by the complex Gaussian distribution whose parameters are respectively given by:*

$$\mathcal{H}_0 : Y_{\mathcal{M}_1} \sim \mathcal{CN}\left(0, \frac{\bar{E}\sigma_h^2 + \sigma_n^2}{N}\right), \tag{6}$$

$$\mathcal{H}_1 : Y_{\mathcal{M}_1} \sim \mathcal{CN}\left(0, \frac{\bar{E}\sigma_h^2\left(1+|\alpha|^2\sigma_h^2\right) + \sigma_n^2}{N}\right). \tag{7}$$

Proof: See Appendix A. ∎

In the case of scheme $\mathcal{M}_2$, the two hypotheses are re-defined based on the actual message data m. The null hypothesis $\mathcal{H}_0$ corresponds to the scenario $m \equiv 0$ while the alternate hypothesis $\mathcal{H}_1$ corresponds to the case of $m \equiv 1$. To transmit the message bits $m \equiv 0$ and $m \equiv 1$, the transmitter device will send codewords $[0\,1]$ or $[1\,0]$, respectively. Therefore, we need to derive the joint conditional distributions of the received signals over the two symbol durations for scheme $\mathcal{M}_2$.

Lemma 2. *The joint PDFs of $Y_{\mathcal{M}_2}[0]$ and $Y_{\mathcal{M}_2}[1]$ conditioned on $\mathcal{H}_0$ and $\mathcal{H}_1$ for the scheme $\mathcal{M}_2$ are given by:*

$$\mathcal{H}_0 : f\left(Y_{\mathcal{M}_2}[0], Y_{\mathcal{M}_2}[1]\right) = \frac{\exp\left\{-\left(\frac{\left|Y_{\mathcal{M}_2}[0]\right|^2}{\frac{\bar{E}\sigma_h^2+\sigma_n^2}{N}} + \frac{\left|Y_{\mathcal{M}_2}[1]\right|^2}{\frac{\bar{E}\sigma_h^2\left(1+|\alpha|^2\sigma_h^2\right)+\sigma_n^2}{N}}\right)\right\}}{\frac{\pi}{N}\sqrt{\left(\bar{E}\sigma_h^2+\sigma_n^2\right)\left(\bar{E}\sigma_h^2\left(1+|\alpha|^2\sigma_h^2\right)+\sigma_n^2\right)}}, \tag{8}$$

$$\mathcal{H}_1 : f\left(Y_{\mathcal{M}_2}[0], Y_{\mathcal{M}_2}[1]\right) = \frac{\exp\left\{-\left(\frac{\left|Y_{\mathcal{M}_2}[0]\right|^2}{\frac{\bar{E}\sigma_h^2\left(1+|\alpha|^2\sigma_h^2\right)+\sigma_n^2}{N}} + \frac{\left|Y_{\mathcal{M}_2}[1]\right|^2}{\frac{\bar{E}\sigma_h^2+\sigma_n^2}{N}}\right)\right\}}{\frac{\pi}{N}\sqrt{\left(\bar{E}\sigma_h^2+\sigma_n^2\right)\left(\bar{E}\sigma_h^2\left(1+|\alpha|^2\sigma_h^2\right)+\sigma_n^2\right)}}. \tag{9}$$

Proof: See Appendix B. ∎

B. Single Antenna Receiver

From the analysis of conditional distributions, we see that PDFs under the two hypotheses have the same mean but different variances. For the scheme $\mathcal{M}_1$, the complex Gaussian PDFs of the two hypotheses derived above are directly compared to obtain the optimal detection threshold. In the case of $\mathcal{M}_2$, the joint distribution of the received mean estimates corresponding to the two symbol durations of the backscatter data are compared to derive the optimal threshold.

Theorem 1. *The average BER of the first encoding scheme $\mathcal{M}_1$ for a single antenna receiver is given by:*

$$P_{\mathcal{M}_1}(e) = \frac{1}{2} - \frac{1}{2}e^{-\frac{T_{\mathcal{M}_1}}{\frac{\bar{E}\sigma_h^2\left(1+|\alpha|^2\sigma_h^2\right)+\sigma_n^2}{N}}} + \frac{1}{2}e^{-\frac{T_{\mathcal{M}_1}}{\frac{\bar{E}\sigma_h^2+\sigma_n^2}{N}}}, \tag{10}$$

where $T_{\mathcal{M}_1} = \frac{\ln\left[\frac{\bar{E}\sigma_h^2\left(1+|\alpha|^2\sigma_h^2\right)+\sigma_n^2}{\bar{E}\sigma_h^2+\sigma_n^2}\right]}{2|\alpha|^2\bar{E}\sigma_h^4}\frac{\left(\bar{E}\sigma_h^2+\sigma_n^2\right)\left(\bar{E}\sigma_h^2\left(1+|\alpha|^2\sigma_h^2\right)+\sigma_n^2\right)}{N}$ is the optimal detection threshold of scheme $\mathcal{M}_1$.

Proof: See Appendix C. ∎

Theorem 2. *The average BER of the second encoding scheme $\mathcal{M}_2$ for a single antenna receiver is given by:*

$$P_{\mathcal{M}_2}(e) = \frac{1}{1 + \frac{\bar{E}\sigma_h^2\left(1+|\alpha|^2\sigma_h^2\right)+\sigma_n^2}{\bar{E}\sigma_h^2+\sigma_n^2}}. \tag{11}$$

Proof: See Appendix D. ∎

Remark 3. *Clearly, the BER expressions of the two described encoding schemes for a single antenna receiver are independent of N. Furthermore, the asymptotic BER values, with respect to the increasing SNR, reach an error floor instead of converging to zero. This can be directly inferred for $\mathcal{M}_2$ because of the simplicity of its BER expression but will also be numerically demonstrated for $\mathcal{M}_1$ in Fig. 1. This necessitates the need for developing better techniques to decode data in a fast fading channel, which takes us to the next main contribution.*

C. Multi-Antenna Receiver

The main reason for the poor BER performance of single antenna receiver is the presence of the direct path from ambient source which only acts as interference since it does not carry any backscatter data. For a multi-antenna receiver, the signal impinging on neighboring antenna element is a phase shifted version of the signal on the first antenna (along with independent additive noise). The signal model of this receiver is represented in (4). Observe that the phase offset of the backscatter link is independent of the phase offset of the direct link. We can remove the direct link by inverting the phase offset of the direct link at the second antenna and subtracting

from the signal at the first antenna. After multiplying the signal at second antenna element by $e^{-j\phi_1}$, we have the following effective signals:

$$\mathcal{H}_0 : y_{\text{eff}}(n) = e^{-j\phi_1} y_1(n) - y_0(n) = \tilde{w}_1(n) - w_0(n),$$
$$\mathcal{H}_1 : y_{\text{eff}}(n) = e^{-j\phi_1} y_1(n) - y_0(n)$$
$$= \alpha h_t(n) h_b(n) x(n)(e^{j(\phi_2-\phi_1)} - 1) + \tilde{w}_1(n) - w_0(n).$$

The average of the effective signal samples $y_{\text{eff}}(n)$ given by $Y = \frac{1}{N}\sum_{n=1}^{N} y_{\text{eff}}(n)$ is used to decode the transmitted data at the multi-antenna receiver. While there are multiple ways of estimating the direct link phase-offset inversion component $e^{-j\phi_1}$, we have provided one in Appendix F.

The effective signal $y_{\text{eff}}(n)$ under $\mathcal{H}_0$ is the difference of two complex Gaussian RVs which again results in a complex Gaussian RV with variance equal to the sum of variances of the two RVs. On the other hand, $y_{\text{eff}}(n)$ under $\mathcal{H}_1$ is a circular symmetric complex RV with zero mean and variance given by:

$$\text{VAR}\left[y_{\text{eff}}|\mathcal{H}_1\right] = \text{VAR}\left[\alpha h_t(n) h_b(n) x(n)(e^{j(\phi_2-\phi_1)} - 1)\right] + \text{VAR}\left[\tilde{w}_1(n) - w_0(n)\right]$$
$$= \left|e^{j\frac{\phi_2-\phi_1}{2}}\right|^2 \left|e^{j\frac{\phi_2-\phi_1}{2}} - e^{-j\frac{\phi_2-\phi_1}{2}}\right|^2 |\alpha|^2 |x(n)|^2 \sigma_h^4 + 2\sigma_n^2$$
$$= 4\sin^2\left(\frac{\phi_2-\phi_1}{2}\right)|\alpha|^2 |x(n)|^2 \sigma_h^4 + 2\sigma_n^2.$$

The mean of received samples Y under $\mathcal{H}_0$ will result in a complex Gaussian RV whose parameters are given below:

$$\mathcal{H}_0 \left\{ Y \sim \mathcal{CN}\left(0, \frac{2\sigma_n^2}{N}\right). \right. \tag{12}$$

Similarly, the mean of received samples Y under $\mathcal{H}_1$ is also shown to be a complex Gaussian using CLT, and the parameters in this case are provided below:

$$\mathcal{H}_1 \left\{ Y \sim \mathcal{CN}\left(0, \frac{4\sin^2\left(\frac{\phi_2-\phi_1}{2}\right)|\alpha|^2 \bar{E}\sigma_h^4 + 2\sigma_n^2}{N}\right). \right. \tag{13}$$

Theorem 3. *The average BER of the first and second encoding schemes in a multi-antenna receiver are respectively given by:*

$$P_{\mathcal{M}_1}(e) = \int_{-\pi}^{\pi}\int_{-\pi}^{\pi} \frac{1}{8\pi^2}\left(1 - e^{-\frac{T_{\mathcal{M}_1}}{s_1}} + e^{-\frac{T_{\mathcal{M}_1}}{s_0}}\right) \mathrm{d}\theta_1 \mathrm{d}\theta_2, \tag{14}$$

$$P_{\mathcal{M}_2}(e) = \int_{-\pi}^{\pi}\int_{-\pi}^{\pi} \frac{1}{2\pi} \times \frac{1}{2\pi} \times \frac{1}{2} \times \frac{\sigma_n^2}{\sin^2\left\{\frac{\pi}{\lambda} d(\cos\theta_2 - \cos\theta_1)\right\}|\alpha|^2 \bar{E}\sigma_h^4 + \sigma_n^2} \mathrm{d}\theta_1 \mathrm{d}\theta_2, \tag{15}$$

where $s_1 = \frac{4\sin^2\left\{\frac{\pi}{\lambda} d(\cos\theta_2 - \cos\theta_1)\right\}|\alpha|^2 \bar{E}\sigma_h^4 + 2\sigma_n^2}{N}$ *and* $s_0 = \frac{2\sigma_n^2}{N}$, *and*

$$T_{\mathcal{M}_1} = \frac{s_1 s_0}{s_1 - s_0} \ln\left(\frac{s_1}{s_0}\right) \tag{16}$$

is the optimal detection threshold of scheme $\mathcal{M}_1$.

Proof: See Appendix E. ∎

IV. Numerical Results

The BER plots of the two encoding schemes $\mathcal{M}_1$ and $\mathcal{M}_2$ for both of the receivers are shown in Fig. 1. We can observe from the figure that with increasing SNR, the BER saturates very quickly for a single antenna receiver. Even changing the encoding scheme from $\mathcal{M}_1$ to $\mathcal{M}_2$ does not offer any noticeable improvement. On the other hand, the multi-antenna receiver can drastically improve the BER of $\mathcal{M}_1$ by removing the interference created by the direct path from the ambient power source. In this case, BER decreases continuously without reaching any error floor. Additionally by using scheme $\mathcal{M}_2$, the multi-antenna receiver can achieve an additional gain of atleast 3dB as shown in the plot.

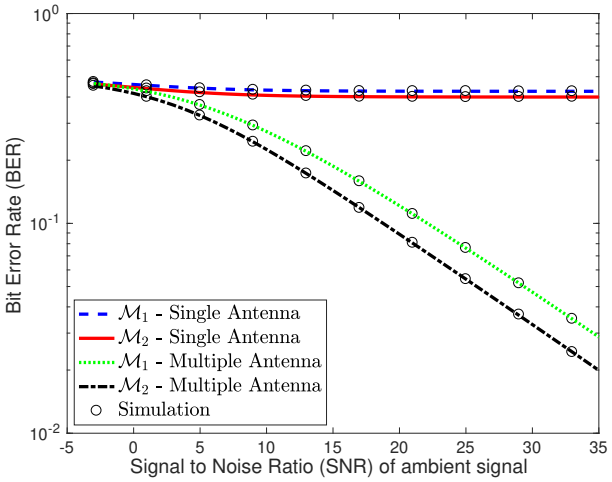

Fig. 1. BER performance of the two encoding schemes for single antenna and multi-antenna receivers.

V. Conclusion

In this paper, we have investigated data encoding and non-coherent detection for ambient backscatter systems in a fast fading channel. The receiver architecture used in the work is based on the average of the received signal samples which removes the dependence of the BER on the signal sample size N. We have shown that a BER floor exists for a single antenna receiver under this architecture due to the interference created by the direct link from the ambient source, which results in an unacceptable performance. We have further shown that this direct link can be eliminated with multiple antennas using the fact that AoA of the direct link can be tracked, thereby resulting in improved BER performance. To the best of our knowledge, this is the first work that presents a comprehensive analytical treatment of non-coherent detection for ambient backscatter under fast-varying channel.

Appendix

A. Proof of Lemma 1

Conditioned on $\mathcal{H}_0$, the signal at the receiver is given by:

$$y(n) = h_r(n)x(n) + w(n),$$

where $h_r(n) \sim \mathcal{CN}\left(0, \sigma_h^2\right)$ and $w(n) \sim \mathcal{CN}\left(0, \sigma_n^2\right)$ are complex Gaussian RVs. Further conditioning on the signal $x(n)$, each received sample in the window length N is an independent complex Gaussian RV whose distribution is $\mathcal{CN}(0, |x(n)|^2\sigma_h^2 + \sigma_n^2)$. The mean of these independent complex Gaussian RVs Y is again a complex Gaussian RV whose distribution is $\mathcal{CN}(0, \frac{\sum |x[i]|^2\sigma_h^2 + N.\sigma_n^2}{N^2})$. Using the assumption in (5), the distribution simplifies to $Y \sim \mathcal{CN}(0, \frac{\bar{E}\sigma_h^2 + \sigma_n^2}{N})$. This distribution turns out to be independent of the symbol sequence

$x(n)$. Similarly, conditioned on $\mathcal{H}_1$, the received signal is given by:

$$y(n) = h_r(n)x(n) + \alpha h_t(n)h_b(n)x(n) + w(n),$$

where $h_r(n), h_t(n)$ and $h_b(n) \sim \mathcal{CN}\left(0, \sigma_h^2\right)$, and $w(n) \sim \mathcal{CN}\left(0, \sigma_n^2\right)$ are complex Gaussian RVs. Further conditioning on signal $x(n)$, each term is an independent circularly-symmetric complex RV with mean 0 and variance $|x(n)|^2\sigma_h^2 + |\alpha|^2|x(n)|^2\sigma_h^4$. From CLT, under the assumption of a large N value, the mean of these independent complex RVs has a distribution $Y \sim \mathcal{CN}(0, \frac{\bar{E}\sigma_h^2\left(1+|\alpha|^2\sigma_h^2\right)+\sigma_n^2}{N})$. This distribution again turns out to be independent of the sequence $x(n)$.

B. Proof of Lemma 2

For the second scheme, the null hypothesis $\mathcal{H}_0$ corresponds to the scenario $b[0] \equiv 0$ and $b[1] \equiv 1$, and the alternate hypothesis $\mathcal{H}_1$ corresponds to the case $b[0] \equiv 1$ and $b[1] \equiv 0$. The respective marginal conditional distributions of the mean of the received signal samples $Y_{\mathcal{M}_2}[0]$ and $Y_{\mathcal{M}_2}[1]$ for the two symbol duration are given by:

$$\mathcal{H}_0 \begin{cases} Y_{\mathcal{M}_2}[0] = \mathcal{CN}\left(0, \frac{\bar{E}\sigma_h^2+\sigma_n^2}{N}\right) \\ Y_{\mathcal{M}_2}[1] = \mathcal{CN}\left(0, \frac{\bar{E}\sigma_h^2(1+|\alpha|^2\sigma_h^2)+\sigma_n^2}{N}\right), \end{cases}$$

$$\mathcal{H}_1 \begin{cases} Y_{\mathcal{M}_2}[0] = \mathcal{CN}\left(0, \frac{\bar{E}\sigma_h^2(1+|\alpha|^2\sigma_h^2)+\sigma_n^2}{N}\right) \\ Y_{\mathcal{M}_2}[1] = \mathcal{CN}\left(0, \frac{\bar{E}\sigma_h^2+\sigma_n^2}{N}\right). \end{cases}$$

Note that $Y_{\mathcal{M}_2}[0]$ and $Y_{\mathcal{M}_2}[1]$ are independent under each of the hypotheses. Therefore, the joint conditional distribution functions can be expressed as the product of the marginal conditional distributions which completes the proof.

C. Proof of Theorem 1

By comparing the conditional PDFs of the two hypotheses derived in Lemma 1, the optimal decision rule of the first encoding scheme is given by:

$$f(Y_{\mathcal{M}_1}|m=0) \gtrless_1^0 f(Y_{\mathcal{M}_1}|m=1)$$

$$\ln(f(Y_{\mathcal{M}_1}|m=0)) \gtrless_1^0 \ln(f(Y_{\mathcal{M}_1}|m=1))$$

$$-\frac{1}{2}\ln\left(\frac{\bar{E}\sigma_h^2+\sigma_n^2}{N}\right) - \frac{|Y_{\mathcal{M}_1}|^2}{\frac{\bar{E}\sigma_h^2+\sigma_n^2}{N}} \gtrless_1^0$$

$$-\frac{1}{2}\ln\left(\frac{\bar{E}\sigma_h^2(1+|\alpha|^2\sigma_h^2)+\sigma_n^2}{N}\right) - \frac{|Y_{\mathcal{M}_1}|^2}{\frac{\bar{E}\sigma_h^2(1+|\alpha|^2\sigma_h^2)+\sigma_n^2}{N}}$$

$$|Y_{\mathcal{M}_1}|^2 \gtrless_0^1 \frac{\ln\left[\frac{\bar{E}\sigma_h^2\left(1+|\alpha|^2\sigma_h^2\right)+\sigma_n^2}{\bar{E}\sigma_h^2+\sigma_n^2}\right]}{2|\alpha|^2\bar{E}\sigma_h^4} \times \frac{\left(\bar{E}\sigma_h^2+\sigma_n^2\right)\left(\bar{E}\sigma_h^2\left(1+|\alpha|^2\sigma_h^2\right)+\sigma_n^2\right)}{N}, \quad (17)$$

where $Y_{\mathcal{M}_1}$ is the mean of the signal samples received for each window slot in the first scheme. The optimal detection threshold $T_{\mathcal{M}_1}$ can be obtained from the decision rule in (17). Observe that the decision rule is dependent on $|Y_{\mathcal{M}_1}|^2$ whose PDF is given by an exponential distribution. The mean of the exponential distribution is related to the variance of the complex Gaussian as follows:

$$X \sim \mathcal{CN}\left(0, \sigma^2\right) \implies |X|^2 \sim \exp\left(\sigma^2\right).$$

Assuming equal prior probabilities for the two hypotheses, the equation for the average BER in this case is given by:

$$P_{\mathcal{M}_1}(e) = P(\mathcal{H}_0)P_{\mathcal{M}_1}(e|\mathcal{H}_0) + P(\mathcal{H}_1)P_{\mathcal{M}_1}(e|\mathcal{H}_1)$$

$$= \frac{1}{2}\left(Pr\left\{|Y_{\mathcal{M}_1}|^2 > T_{\mathcal{M}_1}|\mathcal{H}_0\right\} + Pr\left\{|Y_{\mathcal{M}_1}|^2 < T_{\mathcal{M}_1}|\mathcal{H}_1\right\}\right)$$

$$= 1 - F_{\exp}(T_{\mathcal{M}_1}, \frac{\bar{E}\sigma_h^2+\sigma_n^2}{N}) + F_{\exp}(T_{\mathcal{M}_1}, \frac{\bar{E}\sigma_h^2\left(1+|\alpha|^2\sigma_h^2\right)+\sigma_n^2}{N})$$

$$= \frac{1}{2} - \frac{1}{2}e^{-\frac{T_{\mathcal{M}_1}}{\frac{\bar{E}\sigma_h^2\left(1+|\alpha|^2\sigma_h^2\right)+\sigma_n^2}{N}}} + \frac{1}{2}e^{-\frac{T_{\mathcal{M}_1}}{\frac{\bar{E}\sigma_h^2+\sigma_n^2}{N}}},$$

where $F_{\exp}(x, \lambda) = 1 - e^{-\frac{x}{\lambda}}$ is the cumulative distribution function value of an exponential RV with mean λ at point x.

D. Proof of Theorem 2

By comparing the joint conditional distribution functions, evaluated in Lemma 2, the optimal decision rule of the encoding scheme $\mathcal{M}_2$ can be derived as follows:

$$f\left(Y_{\mathcal{M}_2}[0], Y_{\mathcal{M}_2}[1]|\mathcal{H}_0\right) \gtrless_1^0 f\left(Y_{\mathcal{M}_2}[0], Y_{\mathcal{M}_2}[1]|\mathcal{H}_1\right)$$

$$\ln\left\{f\left(Y_{\mathcal{M}_2}[0], Y_{\mathcal{M}_2}[1]|\mathcal{H}_0\right)\right\} \gtrless_1^0 \ln\left\{f\left(Y_{\mathcal{M}_2}[0], Y_{\mathcal{M}_2}[1]|\mathcal{H}_1\right)\right\}$$

$$-\frac{|Y_{\mathcal{M}_2}[0]|^2}{\frac{\bar{E}\sigma_h^2+\sigma_n^2}{N}} - \frac{|Y_{\mathcal{M}_2}[1]|^2}{\frac{\bar{E}\sigma_h^2(1+|\alpha|^2\sigma_h^2)+\sigma_n^2}{N}} \gtrless_1^0 -\frac{|Y_{\mathcal{M}_2}[0]|^2}{\frac{\bar{E}\sigma_h^2(1+|\alpha|^2\sigma_h^2)+\sigma_n^2}{N}} - \frac{|Y_{\mathcal{M}_2}[1]|^2}{\frac{\bar{E}\sigma_h^2+\sigma_n^2}{N}}$$

$$|Y_{\mathcal{M}_2}[0]|^2 \gtrless_0^1 |Y_{\mathcal{M}_2}[1]|^2. \quad (18)$$

Similar to the first scheme, the optimal decision rule of this scheme is dependent on $|Y_{\mathcal{M}_2}[0]|^2$ and $|Y_{\mathcal{M}_2}[1]|^2$ whose PDFs are given by exponential distributions. Due to the symmetry of the hypotheses, we only need to find error probability for hypothesis $\mathcal{H}_0$. The conditional mean of $|Y_{\mathcal{M}_2}[0]|^2$ and $|Y_{\mathcal{M}_2}[1]|^2$ under null hypothesis are given by $\lambda_0 = \frac{\bar{E}\sigma_h^2+\sigma_n^2}{N}$ and $\lambda_1 = \frac{\bar{E}\sigma_h^2(1+|\alpha|^2\sigma_h^2)+\sigma_n^2}{N}$, respectively. The expression for the theoretical average BER for scheme $\mathcal{M}_2$ can be derived as follows:

$$P_{\mathcal{M}_2}(e) = Pr\left\{|Y_{\mathcal{M}_2}[0]|^2 > |Y_{\mathcal{M}_2}[1]|^2 \mid \mathcal{H}_0\right\}$$

$$= Pr\left\{|Y_{\mathcal{M}_2}[0]|^2 > t \mid |Y_{\mathcal{M}_2}[1]|^2 = t, \mathcal{H}_0\right\}$$

$$= \int_0^\infty \left[1 - F_{\exp}\left(t, \lambda_0\right)\right] f_{\exp}\left(t, \lambda_1\right) \mathrm{d}t$$

$$= \int_0^\infty e^{-\frac{t}{\lambda_0}} \frac{1}{\lambda_1} e^{-\frac{t}{\lambda_1}} \mathrm{d}t = \int_0^\infty \frac{1}{\lambda_1} e^{-t\left(\frac{1}{\lambda_0}+\frac{1}{\lambda_1}\right)} \mathrm{d}t$$

$$= \frac{1}{1+\frac{\lambda_1}{\lambda_0}} = \frac{1}{1+\frac{\bar{E}\sigma_h^2(1+|\alpha|^2\sigma_h^2)+\sigma_n^2}{\bar{E}\sigma_h^2+\sigma_n^2}},$$

where $f_{\exp}(x, \lambda) = \frac{1}{\lambda}e^{-\frac{x}{\lambda}}$ is the PDF value of an exponential RV with mean λ at point x.

E. Proof of Theorem 3

By comparing the conditional PDFs of the two hypotheses given in (12) and (13), the optimal detection threshold $T_{\mathcal{M}_1}$ of the first encoding scheme $\mathcal{M}_1$ can be obtained as given in (16).

The conditional BER is evaluated using a procedure similar to the one used for the average BER in case of a single antenna receiver. The average BER in this case can be evaluated by marginalizing over the range of AoAs θ_1 and θ_2.

For the second scheme $\mathcal{M}_2$, the respective conditional distributions of the mean of the signal samples received for the two window slots $Y_{\mathcal{M}_2}[0]$ and $Y_{\mathcal{M}_2}[1]$ are given by:

$$\mathcal{H}_0 \begin{cases} Y_{\mathcal{M}_2}[0] \sim \mathcal{CN}(0, \frac{2\sigma_n^2}{N}) \\ Y_{\mathcal{M}_2}[1] \sim \mathcal{CN}(0, \frac{4\sin^2\left(\frac{\phi_2-\phi_1}{2}\right)|\alpha|^2\bar{E}\sigma_h^4+2\sigma_n^2}{N}), \end{cases}$$

$$\mathcal{H}_1 \begin{cases} Y_{\mathcal{M}_2}[0] \sim \mathcal{CN}(0, \frac{4\sin^2\left(\frac{\phi_2-\phi_1}{2}\right)|\alpha|^2\bar{E}\sigma_h^4+2\sigma_n^2}{N}) \\ Y_{\mathcal{M}_2}[1] \sim \mathcal{CN}(0, \frac{2\sigma_n^2}{N}). \end{cases}$$

The optimal decision rule after comparing the joint conditional distribution functions is again given by (18). The expression for conditional BER can be derived as follows:

$$\begin{aligned} P_{\mathcal{M}_2}(e|\phi_1,\phi_2) &= \frac{1}{1+\frac{4\sin^2\left(\frac{\phi_2-\phi_1}{2}\right)|\alpha|^2\bar{E}\sigma_h^4+2\sigma_n^2}{2\sigma_n^2}} \\ &= \frac{\sigma_n^2}{2\sin^2(\frac{\phi_2-\phi_1}{2})|\alpha|^2\bar{E}\sigma_h^4+2\sigma_n^2}. \end{aligned} \quad (19)$$

We can observe from the above expression that the conditional BER approaches zero at higher values of SNR. The above expression is dependent on the difference between the phase-offsets of the two links. To understand the average performance of the detection mechanism, we can average over the range of phase-offset values. For a linear uniform antenna array, the phase offset is related to AoA θ by the relation $\phi = \frac{2\pi}{\lambda} d\cos\theta$. The assumption is that the AoAs of the direct link θ_1 and the backscatter link θ_2 are identical, independent and uniformly distributed over the range $(-\pi, \pi]$. Marginalizing over the range of θ_1 and θ_2 we get the expression as given in (15).

F. Estimation of phase offset of direct path

We can determine the phase-offset inversion component of the direct RF link at the receiver using the following approach. When message bit of value 0 is transmitted, the received signal at the two antenna elements is given by:

$$\mathbf{y}(n) = \begin{bmatrix} y_0(n) \\ y_1(n) \end{bmatrix} = h_r(n) \begin{bmatrix} 1 \\ e^{j\phi_1} \end{bmatrix} x(n) + \begin{bmatrix} w_0(n) \\ w_1(n) \end{bmatrix},$$

Taking the summation of samples of block length N, we get the following:

$$\begin{aligned} \sum \mathbf{y}(n) &= \begin{bmatrix} \sum y_0(n) \\ \sum y_1(n) \end{bmatrix} = \sum h_r(n)x(n) \begin{bmatrix} 1 \\ e^{j\phi_1} \end{bmatrix} + \begin{bmatrix} \sum w_0(n) \\ \sum w_1(n) \end{bmatrix} \\ &= c_0 \begin{bmatrix} 1 \\ e^{j\phi_1} \end{bmatrix} + \begin{bmatrix} n_0 \\ n_1 \end{bmatrix}, \end{aligned}$$

where $c_0 \sim \mathcal{CN}(0, N\bar{E}\sigma_h^2)$, $n_0 \sim \mathcal{CN}(0, N\sigma_n^2)$ and $n_1 \sim \mathcal{CN}(0, N\sigma_n^2)$ are independent Gaussian random signals.

Taking cross-correlation of $\sum y_0(n)$ and $\sum y_1(n)$, we get:

$$\begin{aligned} &\mathbb{E}\left[\sum y_0(n) \sum y_1^*(n)\right] \\ &= \mathbb{E}\left[|c_0|^2\right] e^{-j\phi_1} + \mathbb{E}\left[c_0 n_1^*\right] + \mathbb{E}\left[c_0^* e^{-j\phi_1} n_0\right] + \mathbb{E}\left[n_0 n_1^*\right] \\ &= N\bar{E}\sigma_h^2 e^{-j\phi_1} \\ &\implies e^{-j\phi_1} = \frac{\mathbb{E}\left[\sum y_0(n) \sum y_1^*(n)\right]}{N\bar{E}\sigma_h^2}. \end{aligned} \quad (20)$$

REFERENCES

[1] J. K. Devineni and H. S. Dhillon, "Ambient backscatter systems: Exact average bit error rate under fading channels," *IEEE Trans. Green Commun. and Networking*, vol. 3, no. 1, pp. 11–25, Mar. 2019.

[2] K. Lu, G. Wang, F. Qu, and Z. Zhong, "Signal detection and BER analysis for RF-powered devices utilizing ambient backscatter," *Proc., Intl. Conf. on Wireless Commun. & Sig. Proc. (WCSP)*, Oct. 2015.

[3] G. Wang, F. Gao, Z. Dou, and C. Tellambura, "Uplink detection and BER analysis for ambient backscatter communication systems," *Proc., IEEE Globecom*, Dec. 2015.

[4] G. Wang, F. Gao, R. Fan, and C. Tellambura, "Ambient backscatter communication systems: Detection and performance analysis," *IEEE Trans. Commun.*, vol. 64, no. 11, pp. 4836 – 4846, Nov. 2016.

[5] J. Qian, F. Gao, G. Wang, S. Jin, and H. Zhu, "Semi-coherent detection and performance analysis for ambient backscatter system," *IEEE Trans. Commun.*, vol. 65, no. 12, Dec. 2017.

[6] ——, "Noncoherent detections for ambient backscatter system," *IEEE Trans. Wireless Commun.*, vol. 16, no. 3, Mar. 2017.

[7] Y. Liu, Z. Zhong, G. Wang, and D. Hu, "Uplink detection and BER performance for wireless communication systems with ambient backscatter and multiple receiving antennas," *Proc., Intl. Conf. on Commun. and Networking in China (ChinaCom)*, pp. 79 – 84, Aug. 2015.

[8] T. Zeng, G. Wang, Y. Wang, Z. Zhong, and C. Tellambura, "Statistical covariance based signal detection for ambient backscatter communication systems," *Proc., IEEE Veh. Technology Conf. (VTC)*, Sep. 2016.

[9] G. Yang, Y.-C. Liang, R. Zhang, and Y. Pei, "Modulation in the air: Backscatter communication over ambient OFDM carrier," *IEEE Trans. Commun.*, vol. 66, no. 3, pp. 1219–1233, Mar. 2017.

[10] M. A. El Mossallamy, M. Pan, R. Jäntti, K. G. Seddik, G. Y. Li, and Z. Han, "Noncoherent backscatter communications over ambient OFDM signals," *IEEE Trans. Commun.*, vol. 67, no. 5, pp. 3597–3611, Feb. 2019.

[11] Q. Tao, C. Zhong, H. Lin, and Z. Zhang, "Symbol detection of ambient backscatter systems with manchester coding," *IEEE Trans. Wireless Commun.*, vol. 17, no. 6, pp. 4028–4038, Apr. 2018.

[12] Y. Liu, G. Wang, Z. Dou, and Z. Zhong, "New coding and detection schemes for ambient backscatter communication systems," *IEEE Access*, vol. 5, pp. 4947–4953, Mar. 2017.

[13] D. Tse and P. Viswanath, *Fundamentals of wireless communication*. Cambridge university press, 2005.

[14] J. K. Devineni and H. S. Dhillon, "Non-coherent detection and bit error rate for an ambient backscatter link in time-selective fading," *arXiv preprint, arXiv:1908.05657*, 2019.

[15] A. Adhikary, J. Nam, J.-Y. Ahn, and G. Caire, "Joint spatial division and multiplexing-the large-scale array regime," *IEEE Trans. Information Theory*, vol. 59, no. 10, pp. 6441–6463, Jun. 2013.

[16] A. Adhikary, E. Al Safadi, M. K. Samimi, R. Wang, G. Caire, T. S. Rappaport, and A. F. Molisch, "Joint spatial division and multiplexing for mm-wave channels," *IEEE J. Sel. Areas Commun.*, vol. 32, no. 6, pp. 1239–1255, May 2014.

[17] A. Adhikary, H. S. Dhillon, and G. Caire, "Massive-mimo meets hetnet: Interference coordination through spatial blanking," *IEEE J. Sel. Areas Commun.*, vol. 33, no. 6, pp. 1171–1186, Mar. 2015.

[18] F. Fuschini, C. Piersanti, F. Paolazzi, and G. Falciasecca, "Analytical approach to the backscattering from UHF RFID transponder," *IEEE Antennas and Wireless Propagation Letters*, vol. 7, pp. 33–35, Feb. 2008.

[19] C. A. Balanis, *Antenna Theory: Analysis and Design*. John Wiley & Sons, 2005.

[20] A. Bletsas, A. G. Dimitriou, and J. N. Sahalos, "Improving backscatter radio tag efficiency," *IEEE Trans. Microwave Theory Tech*, vol. 58, no. 6, pp. 1502–1509, Jun. 2010.